

# Extracting meteorological influence from ionospheric disturbances

P. Hoffmann, Ch. Jacobi

## Summary:

The state and variability of the thermosphere/ionosphere system can be described by the total electron content (TEC). The solar forcing through ionisation is dominant. But there are transport processes of the ionized plasma through thermospheric wind systems which cause anomalies in the behaviour of the electron density. An important question in this context is, whether signals of planetary waves (PW) from middle atmosphere may be detected in ionospheric disturbances of the total electron content. A direct penetration of PW into the thermosphere is not possible, but indirect mechanism of modulation of solar tides are not debarred. Thus, the analysis of hemispheric TEC-maps in combination to stratospheric reanalysis data and other atmospheric measurements may help to investigate the problem of vertical coupling.

This study presents signatures of winter stratospheric planetary waves visible in the ionospheric TEC. The westward propagating component having zonal wavenumber 1 reveals a correspondence between the stratosphere and ionosphere for periods of quasi 16-, 7- and 4-days close to the atmospheric normal modes.

## Zusammenfassung:

Der Zustand und die Variabilität des Systems der Thermosphäre/Ionosphäre lassen sich durch den totalen Elektronengehalt (TEC) beschreiben. Wenn gleich der solare Antrieb durch Ionisation überwiegt, gibt es Transportprozesse des ionisierten Plasma durch thermosphärische Windsysteme, welche Anomalien in der Elektronendichte verursachen. Eine in diesem Zusammenhang wichtige Frage ist, ob sich Signale planetarer Wellen der mittleren Atmosphäre in ionosphärischen Störungen im Gesamtelektronengehalt finden lassen. Eine direkte Ausbreitung planetarer Wellen (PW) in die Thermosphäre ist nicht möglich, aber indirekte Mechanismen wie die Modulation durch solare Gezeiten werden nicht ausgeschlossen. Deshalb werden hier Analysen von hemisphärischen TEC-Karten in Kombination mit stratosphärischen Reanalyse-Daten und anderen atmosphärischen Messungen durchgeführt, um das Problem der vertikalen Koppelung zu untersuchen.

Diese Studie hier zeigt, dass sich Signaturen von stratosphärischer planetarer Wellenaktivität im Winter auch im ionosphärischen TEC abbilden. Die westwärtswandernde Komponente mit Wellenzahl 1 zeigt offenbar eine gute Übereinstimmung zwischen der Stratosphäre und Ionosphäre mit Perioden von quasi 16-, 7-, 4-Tagen, welche nahe denjenigen der atmosphärischen Normalmoden liegen.

# 1 Introduction

A global picture of the thermosphere dynamics, including the neutral component of the upper atmosphere above 100 km, is still not well developed. Spectrometers on satellites (e.g. SABER on TIMED) may only scan the atmosphere orbit per orbit resulting a global monthly mean picture of meteorological parameters. Other work is ground based like radar and ionosonde. They have a high temporal resolution but only a well developed network can deliver a hemispheric image of upper atmosphere dynamics. Information of thermosphere climatology and variability can be indirectly derived from the ionized component, which behaves to a certain degree like a tracer in the local wind system. The paramount production of ions and free electrons is caused by the solar EUV radiation in the ionospheric F-region. The ionized plasma is able to modify radio wave propagation of commercial communication systems. This property is used to gain information about the variability of the thermosphere/ionosphere system. Signals of the Global Navigation System Satellites (GNSS) and a worldwide net of ground base receivers are regularly used by the DLR Neustrelitz since 2002 (Jakowski, 1996) for constructing hemispheric maps of the total electron content (TEC). Such procedure allows monitoring with hourly and reasonable spatial resolution. The ionosphere is mainly forced by the solar radiation. This fact is well visible by comparing the electron density with the solar flux index. Beneath the strong diurnal cycle, the solar rotation period and the solar cycle dependency is observed.

Also signals of middle atmospheric planetary waves (PW) with periods of 2-, 5-, 10-, 16-days, as theoretically predicted by Salby (1984), are expected in the ionospheric disturbances of the total electron content. These waves transfer meteorological information from the troposphere to the middle atmosphere and can be analysed e.g. from global stratospheric reanalysis data, which are regularly produced by UK Met Office since 1991 (Swinbank and O'Neill, 1994) up to  $0.1hPa$  and provided by the British Atmospheric Data Center (BADC). The penetration of PW into the lower thermosphere can only happen indirectly e.g. through the mechanism of modulation. Candidates of carrier could be the semi-diurnal tide (SDT) amplitude and gravity waves (GW) as well as the Electrojet. In Forbes (2000) a general overview of ionospheric variability is given. The interaction of PW with solar tides (12-, 24-h) as well as GW, both became important in the mesosphere/lower thermosphere (MLT), seems to play an essential role in the vertical coupling as suggested by Pancheva et al. (2002) and Lastovicka (2006). Other studies have already shown a simultaneous observation of PW type oscillations (PWTO) in ionospheric parameters and MLT wind (e.g. Altadill, 2003) and stratosphere (Gordienko et al., 2005, Borries et al., 2007). They found an ionospheric signal close to 5- and 10-day periods in coincidence with winter stratospheric PW activity.

The modelling of the middle atmospheric circulation is well developed. Under monthly mean climatological background conditions several studies of PW propagation and interaction with tidal waves and the influence of GW effects can be done. Natural oscillations in the ionosphere-thermosphere-mesosphere (ITM) system were already simulated by Meyer (1997) to identify the spectral response to lower boundary forcing using a Global Scale Wave Model (GSWM) developed by Hagan et al. (1993). Typical peaks near 2-, 5-, 10- and 16- days at lower atmosphere were not present in the ITM system, instead periods similar to gravitational normal modes having several hours for east- and westward propagating waves were theoretically observed. Further experiments using an extended version of a middle atmosphere model including the upper atmosphere (MUAM) are performed by Pogoreltsev (2007) and Jacobi et al. (2007). The results show that stationary and long-period PW are not able to penetrate directly into the thermosphere, but short-period PW (e.g. ultra-fast Kelvin waves and secondary waves) can reach lower thermospheric heights.

The main goal of this study is the investigation of coupling between the middle and upper at-

mosphere to obtain a climatology of variability of the thermosphere/ionosphere system excluded from solar- and geomagnetic influence. Data from northern hemispheric TEC-maps, in this study at  $52.5^\circ N$ , of the years 2002 to 2005 will be analysed with respect to PWTO in comparison to stratospheric reanalysis fields. Local measurements of neutral wind near mesopause region shall fill the huge data gap between stratosphere and ionosphere and help to interpret the results.

## 2 Analysis tools

The work with global data and time series of several atmospheric parameters requires a large extent of accurateness. A mathematical filter routine and a spectral transformation are applied to separate useful signals from noise. For ionospheric correction the hourly time series of  $TEC$  and the critical plasma frequency  $f_oF2$  are averaged over each day and lowpass filtered using the SVDFIT (see numerical recipes) algorithm of least-squares curve fitting. As the basis harmonic functions are used. Oscillations lower than 20 days are filtered out and the new time series, which mainly consists of long-period oscillations of the solar period and the solar cycle, is used as a reference curve. In a following step a differential value is calculated from the difference between the observation and reference and is normalised by the reference, see step 0 in Tab. 1. This new value is almost excluded from the long-period solar effects in  $TEC$ .

To analyse the variability in time series for several period bands a Lanczos filter is applied. A typical period range of 3-10 days and 10-20 days shall represent short- and long-period oscillations. A period-time image of time series is obtained by calculating Morlet wavelet spectra (Torrence, 1998) and the seasonal variability of periodicities between several days can be investigated.

Global data (stratospheric reanalysis data, ionospheric TEC maps) are analysed using the spectral decomposition in the space and time domain for a fixed latitudinal circle (preferring mid-latitude) and at fixed pressure level. The principle was first given by Hayashi (1971) and modified by Pogoreltsev (2002). A short description of the applied method is given by Hoffmann (2007), but will be also given here in more detail. As shown in Tab.1, the data base which cover the longitudinal- and time domain are first decomposed into the zonal harmonics for wavenumber ( $k=0,1,2,3$ ) and the coefficients are estimated for each time segment using least-square approximation applying the singular value decomposition (SVD). The real ( $C_k$ ) and imaginary ( $S_k$ ) parts represent the longitudinal state of the wave at  $\lambda = 0^\circ$  and  $\lambda = 90^\circ/k$  (1st step). A running 48-day window Fourier transform of these both time series results again two coefficients, whereas the real ( $C_c, C_s$ ) and imaginary ( $S_c, S_s$ ) parts describe the state of the wave at time  $t = 0$  and  $t = T/4$ .  $T$  is equal to the wave period and  $T/4$  corresponds to the phase shift between the sine- and cosine function. Possible trends in time series are estimated through a polynomial of order lower than three and a Hanning window is used to reduce the signal noise caused through the limited time segment (2nd step in Tab. 1). To obtain a period-wavenumber (PK) spectrum for one time window a set of equations, given the 3rd step on Tab. 1, has to be solved in which the coefficients for the eastward ( $C_e, S_e$ ) and westward ( $C_w, S_w$ ) propagating waves are searched. This procedure is equivalent to the cross-spectral analysis. The amplitude of stationary components is calculated from the window mean of the two time series ( $C_{stat}, S_{stat}$ ). In step 4 the spectral information of each separated wave is transformed back into the time domain followed by a wavelet transform for the westward- and eastward travelling component (step 5) to exclude the standing part, which is specified by the coherence of east- and westward propagating wave parts. In Pogoreltsev (2007) the difference of both travelling components is used for calculating new amplitudes for the pure east- and westward propagating waves ( $A'_w, A'_e$ ).

GLOBAL GRIDDED DATA	
STRATOSPHERE	IONOSPHERE

**0. TEC CORRECTION:**

$$DTEC = 100\% \cdot \frac{TEC_{obs} - TEC_{ref}}{TEC_{ref}}$$

$$w(\lambda, t)$$

**1. ZONAL HARMONICS:**

*Singular Value Decomposition (SVD)*

$$C(k, t), S(k, t)$$

$$w(\lambda, t) = k_0 + \sum_k C_k(t) \cdot \cos(k\lambda) + S_k(t) \cdot \sin(k\lambda)$$

**2. TEMPORAL HARMONICS:**

*48 days window Fourier transform (WFT)*

$$C_c(k, \omega), C_s(k, \omega), S_c(k, \omega), S_s(k, \omega)$$

$$C_k(t) = C_{stat} + \sum_{\omega} C_{k,\omega} \cdot \cos(\omega t) + S_{k,\omega} \cdot \sin(\omega t)$$

$$S_k(t) = S_{stat} + \sum_{\omega} C_{k,\omega} \cdot \cos(\omega t) + S_{k,\omega} \cdot \sin(\omega t)$$

**3. CROSS-SPECTRAL ANALYSIS:**

$$C_w(k, \omega), C_e(k, \omega), S_w(k, \omega), S_e(k, \omega)$$

$$C_w = +0.5 \cdot (C_c + S_s)$$

$$S_w = -0.5 \cdot (C_s - S_c)$$

$$C_e = +0.5 \cdot (C_c - S_s)$$

$$S_e = +0.5 \cdot (C_s - S_c)$$

**4. BACK TRANSFORM INTO THE TIME DOMAIN**

$$A_w(k, t) = \sum_{\omega} A_w(k, \omega) \cdot \cos(\phi_w(k, \omega))$$

**5. WAVELET SPECTRA:**

*Standing wave exclusion*

$$A'_w(k, \omega), A'_e(k, \omega)$$

$$A'_w = A_w - A_e \quad (A_w > A_e)$$

Table 1: Scheme of the space-time analysis method for planetary wave separation.

### 3 The regular variability of the Ionosphere

The international reference model of the ionosphere (IRI) describes the behaviour of the ionosphere depending extraterrestrial parameters (Bilitza, 1990). The molecular composition of the thermosphere is given by the MSIS climatology based on mass spectrometer incoherent scatter measurements. The solar- and geomagnetic activity indices essentially quantify the production of ions. Beneath the diurnal cycle, the solar rotation period (27-days) and the solar cycle (11-years) dependency, a seasonal anomaly in TEC shows the influence of the thermospheric wind system on the ion content. The meridional circulation directed from the summer to the winter hemisphere causes the maximum in the electron density during winter, despite the lower zenith angle of the sun.

The first study of PWTO analysed from ionospheric TEC maps was applied by Borries et al. (2007).

As a reference to calculate a differential TEC ( $DTEC$ ), a monthly median TEC ( $TEC_{ref}$ ) is specified for every zonal grid point. This procedure removes all stationary effects, and discontinuities occur to the monthly changing reference.

An alternative for excluding long-period solar influence on ionospheric parameter time series ( $TEC$ ,  $foF2$ ) uses a lowpass filter, based on SVDFIT algorithm. The reduction of the diurnal cycle magnitude must be done carefully due to modulation effects.

The basis for calculating the differential TEC ( $DHTEC$ ) is a lowpass filter reference curve from daily-longitude average, applied for every spatial grid point. Instead of the difference the absolute value is used to calculate the differential value, which reduces the diurnal cycle influence.

Another idea hides behind the differential TEC ( $DPTEC$ ). The transformation of the longitudinal grid to the local time domain of hourly TEC data and averaging over one day describes the daily prevailing behaviour.

Furthermore, a differential TEC calculated from a model TEC ( $MTEC$ ) or from an excluded diurnal cycle TEC ( $CTEC$ ) are possible, but are not considered in this study.

Figure 1 depicts the TEC image at mid-latitudes ( $52^\circ N$ ) in the longitude-time domain before (left panels) and after normalisation (right panels). The original data based on from GPS measurements ( $TEC$ ), calculation by IRI ( $MTEC$ ) and transformation into the local time domain ( $PTEC$ ). The solar cycle dependency is well visible in TEC data from 2002 to 2005, which is almost eliminated in the normalised values in the right panel ( $DTEC$ ,  $DHTEC$ ,  $DPTEC$ ). The annual cycle in  $DHTEC$ ,  $DPTEC$  remain conserved, while the  $DTEC$  shows only a weak seasonal structure in the time-longitude image. Probably, the differential TEC of hourly value with a dominating diurnal cycle eliminates all stationary effects.

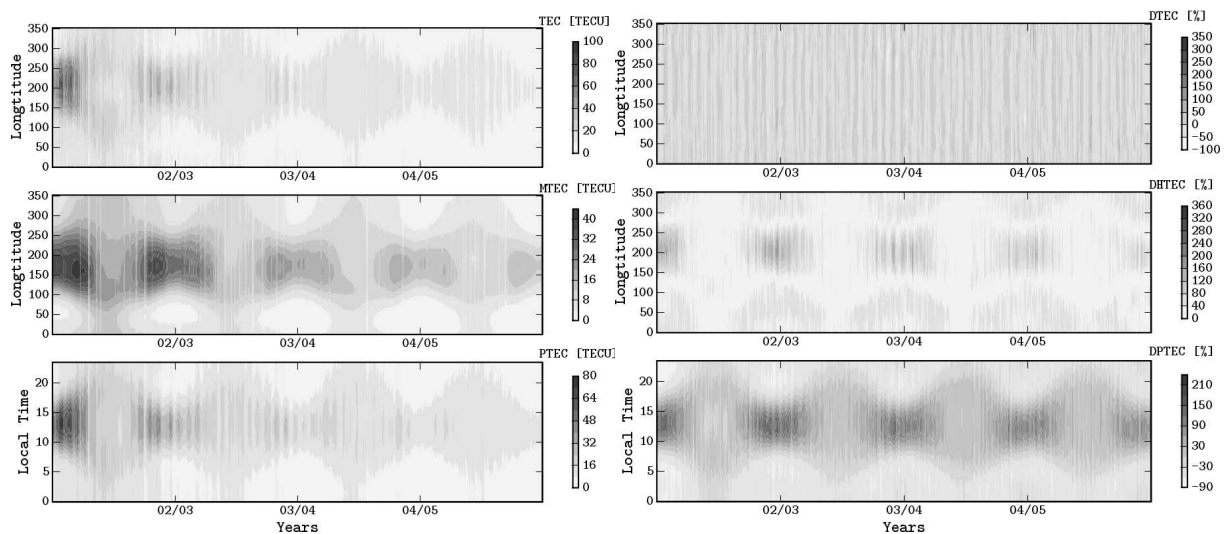


Figure 1:

Left: The longitude-time images over  $52^\circ N$  from 2002 to 2005 show the TEC of GPS ( $TEC$ ), the model TEC ( $MTEC$ ) and the ( $PTEC$ ), which was transformed into the local time domain.

Right: The same as the left panels for the corrected TEC data. The upper panel represents the  $DTEC$  based on monthly median. The middle panel show the  $DHTEC$  using a lowpass filter and the lower one depicts the  $DPTEC$  from local time transform.

## 4 Climatology of middle atmospheric planetary waves

The PW activity in the stratosphere shows a regular behaviour essentially dependent on the zonal background flow. During westerly (eastward) wind in winter the PW are able to propagate into the mesosphere, while easterly (westward) wind impede this process. If the phase speed of PW is equal to the background wind, a penetration into the stratosphere is blocked similar to the mesopause condition. Figure 2 (upper panel) describes the seasonal variability of midlatitudinal stratospheric zonal wind and temperature up to 0.3 hPa using Uk Met Office reanalysis data of 2002 and 2003. The zonal standard deviation is plotted in the lower panel as an indication of variability. This shows disturbances of the winter stratosphere through PW activity. Single stratospheric warming events in winter are also visible in temperature and zonal wind, which reverses direction for a short time. A space-time analysis of PW is shown in Fig.7 (left panel) of chapter 5. The averaged period-wavenumber image of travelling PW at 1 hPa gives the spectrum of stratospheric PW. They are predominately westward propagating having zonal wavenumber 1 with periods of quasi 4-, 7-, 16-days.

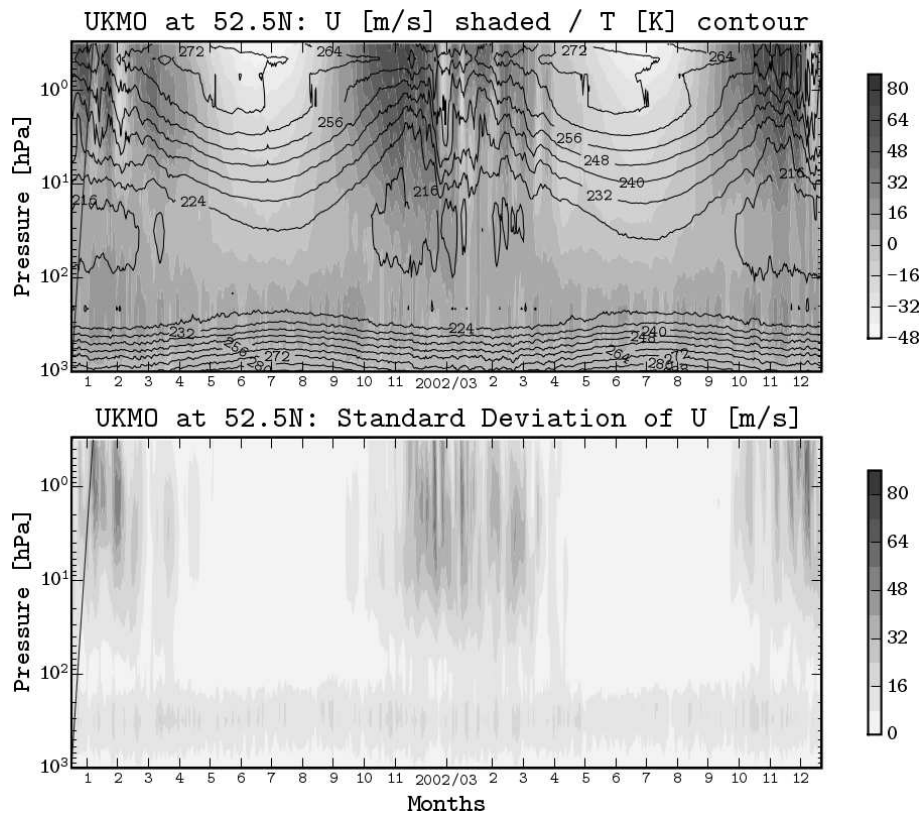


Figure 2: Height-time cross-section of stratospheric reanalyzed zonal wind (shaded) and temperature (contour) in vertical range from 1000 hPa to 0.3 hPa and the time interval starting 2002 to 2005 taken from UKMO.

The mesosphere region is strongly influenced through upward propagating GW from the troposphere. Their wave amplitudes grow with height, break and lead to turbulences, small-scale mixing and dissipation in the upper mesosphere region. GW tend to drag the mean flow and influence the penetration of PW into the thermosphere. Short-period PW are generally strong in summer, while

long-period PW dominate in winter (Beard et al. 2001). But similarities can be found during winter, when a direct wave propagation is possible. Also the cyclic modulation of tidal amplitudes with periods to those of PW is supported in this study. The quasi two-day wave, known as a phenomenon of the summer mesopause, was already numerical studied by Jacobi et al. (2006) using a simple general circulation model. Its modulation of GW fluxes and the consequences of PW propagation are investigated.

## 5 Wave activity in the stratosphere/ionosphere system

Simultaneous observations of wave type oscillations over an altitude range from the stratosphere to the ionosphere and several atmospheric parameters (e.g.  $U$ ,  $f_oF2$ ,  $TEC$ ) as well as extra-terrestrial indices for solar- and geomagnetic activity are first spectrally analysed.

Figure 3 shows the unfiltered time series from 2002 to 2005 at  $52^\circ\text{N}/12^\circ\text{E}$ . The external forcing of ionospheric variability is observed by the solar flux  $F10.7$  and the geomagnetic activity index  $ap$  (A). The decrease of the solar flux during that time corresponds to the 11-year solar cycle and this behaviour is also visible in the response of the ionospheric  $TEC$  of GPS and the  $MTEC$  calculated using the IRI model (B). Single storm events are visible in the response of the ionosphere, too (e.g. early winter 2004). Further analysis of wave type oscillations, a differential  $TEC$  ( $DTEC$ ) is used, which is excluded from solar influence (C). This implicates that the seasonal and annual variability becomes dominant comparable to the neutral wind. The critical plasma frequency  $f_oF2$  measured by ionosondes, but only available for 2004 and 2005, is also corrected from solar effects by introducing a relative value  $df_oF2$  (D). The information of the neutral atmosphere below 100 km is covered by wind measurements in MLT region using the LF-radar  $U_{LF}$  and meteor radar  $U_{MR}$  (E) and the stratospheric data are taken from UK Met Office reanalysis data  $U_{1hPa}$  (F).

The strong annual cycle of the stratospheric zonal wind component is an indicator for stationary planetary wave (SPW), which are modulated by winter PW activity. In comparison to the mesopause region the annual cycle is weaker and modulated by PW in summer. As mentioned in the previous section the behaviour of PW changes through interaction with GW and tides as well as baroclinic instability causes the forcing of PW in the mesosphere.

Dependent on the used  $TEC$  normalisation method the annual cycle is once filtered out (e.g.  $DTEC$ ). Nevertheless, in both cases a seasonal variability of wave signatures is observed in the ionosphere, which is mainly caused by the thermospheric meridional circulation directed from the summer to the winter hemisphere.

The following step applies two several bandpass filter (3-10 days, 10-20 days) for 2005 (Figure 4). The results for the ionosphere show that probably the short-period range modulates the annual cycle. The calculated wavelet spectra in Figure 5 confirm the assumption of ionospheric coupling from below, see the good agreement of the different spectra. Long-period oscillations greater 10-days maximize in winter, while the wave activity in summer is weak through the whole atmospheric layers. The comparison of wavelet spectra for the stratosphere ( $U_{1hPa}$ ), mesosphere/lower thermosphere ( $U_{MR}$ ) and ionosphere ( $DTEC$ ,  $df_oF2$ ) lets suppose the propagation of a quasi 16-day wave signature from the winter stratosphere to the summer ionosphere.

The results from the space-time analysis show a signal of SPW1 in the corrected ionospheric  $DHTEC$  and  $DTEC$  in good correspondence to the stratosphere (Fig. 6). In  $DTEC$  the stationary part is not visible.

An averaged picture of the travelling wave components is shown in Figure 7. The amplitude of the east- and westward propagating waves in the ionosphere are similar in contrast to the dominant

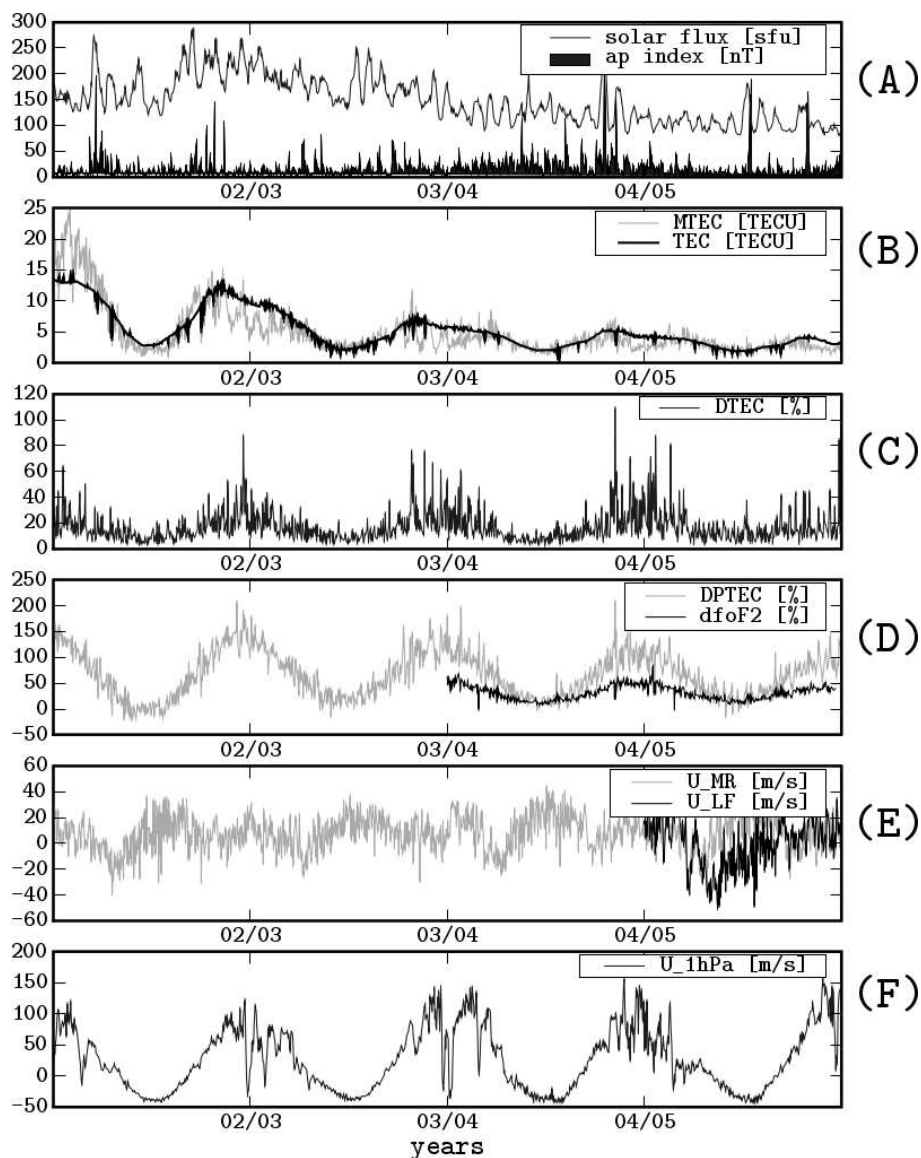


Figure 3: Unfiltered time series of local observations at  $52^{\circ}N/12^{\circ}E$  from 2002 to 2005 for different altitudes up to 300 km. The used data are enumerated starting from above: F10.7, Ap (A) TEC, MTEC (B) DTEC (C) DPTEC,  $df_oF2$  (D)  $U_{MR}$ ,  $U_{LF}$  (E)  $U_{1hPa}$  (F).

westward propagating stratospheric PW having zonal wavenumber  $k=1$  and periods of quasi 4-, 7-, and 16-days. A dominating period in the mean spectra of the ionosphere does not exist. The amplitudes for the zonal mean oscillation is the most dominant type. A 5-day wave signature of  $k=0$  is visible in both  $DTEC$  and  $DHTEC$ .

Figure 8 displays the wavelet spectra of the difference between west- and eastward ( $A_w - A_e$ ) propagating waves in the stratosphere and ionosphere. This procedure is applied for eliminating the standing waves from the travelling components. The results for the pure westward propagating wave signature ( $A'_w$ ) having zonal wavenumber 1 in the ionosphere is in very good agreement with the behaviour of this wave type in the winter stratosphere. Quasi 4-, 7-, 16-day signatures are visible in both averaged spectra.

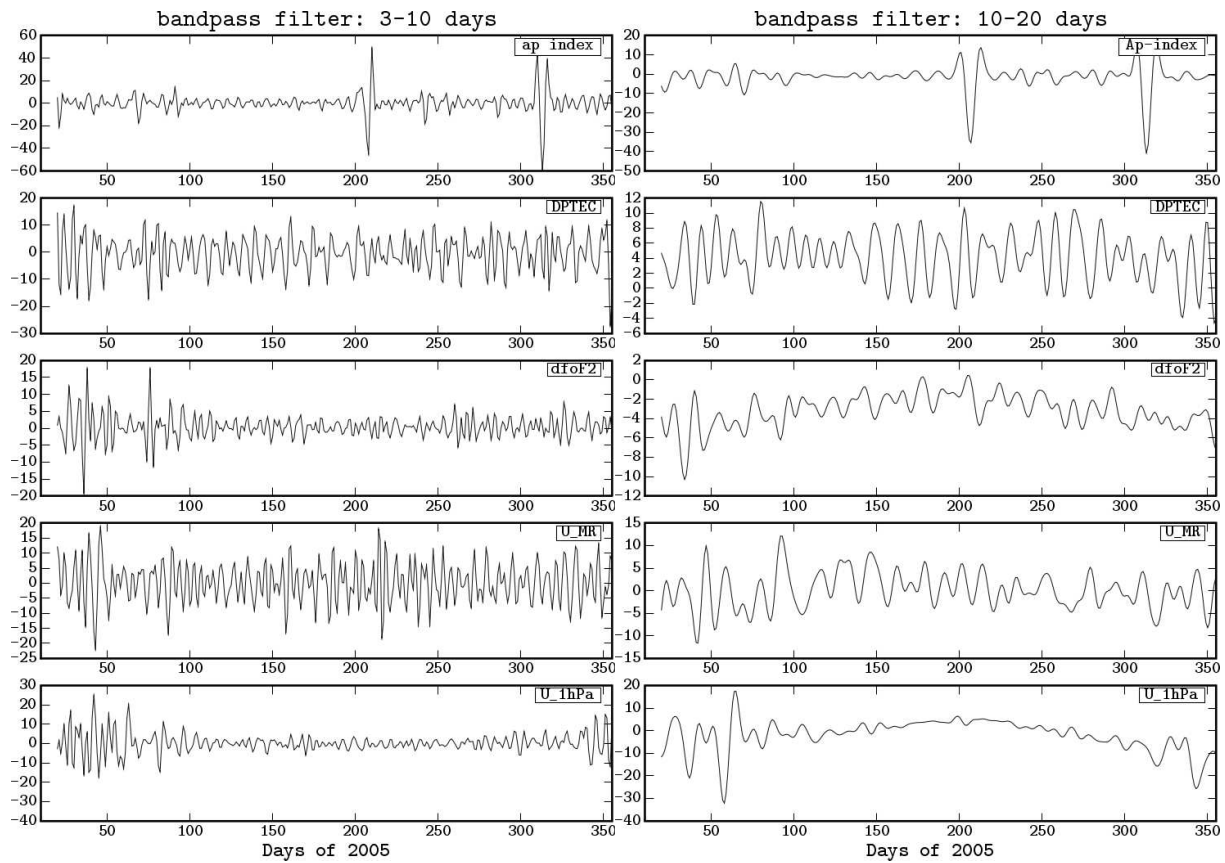


Figure 4: Bandpass filtered time series of 2005 for the period range 3-10 days (left) and 10-20 days (right) using the following data:  $A_p$ , DPTEC,  $df_oF2$ ,  $U_{MR}$ ,  $U_{1hPa}$

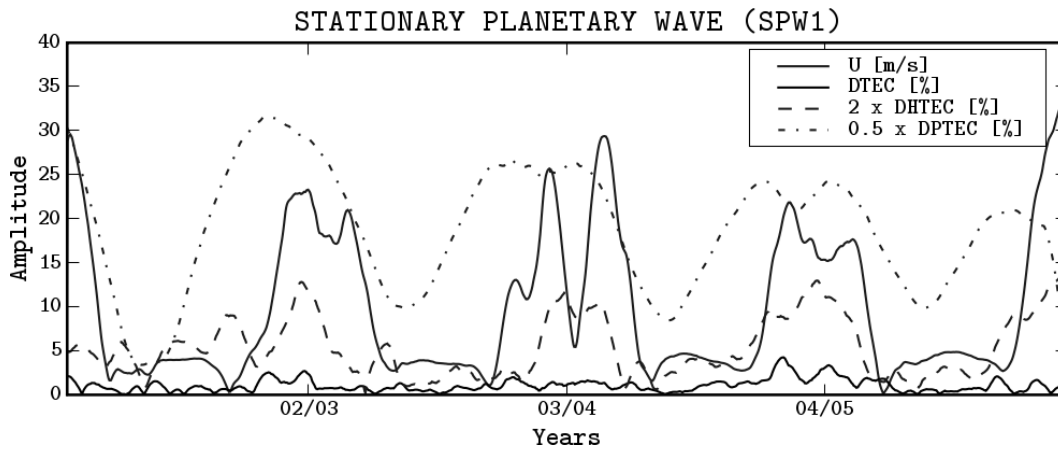


Figure 6: Time series of the stationary planetary wave (SPW) amplitudes for zonal wavenumber ( $k = 1$ ) analysed from the stratosphere ( $U_{1hPa}$ ) and in comparison to several ionospheric differential TEC corrections (DTEC, DHTEC, DPTEC).

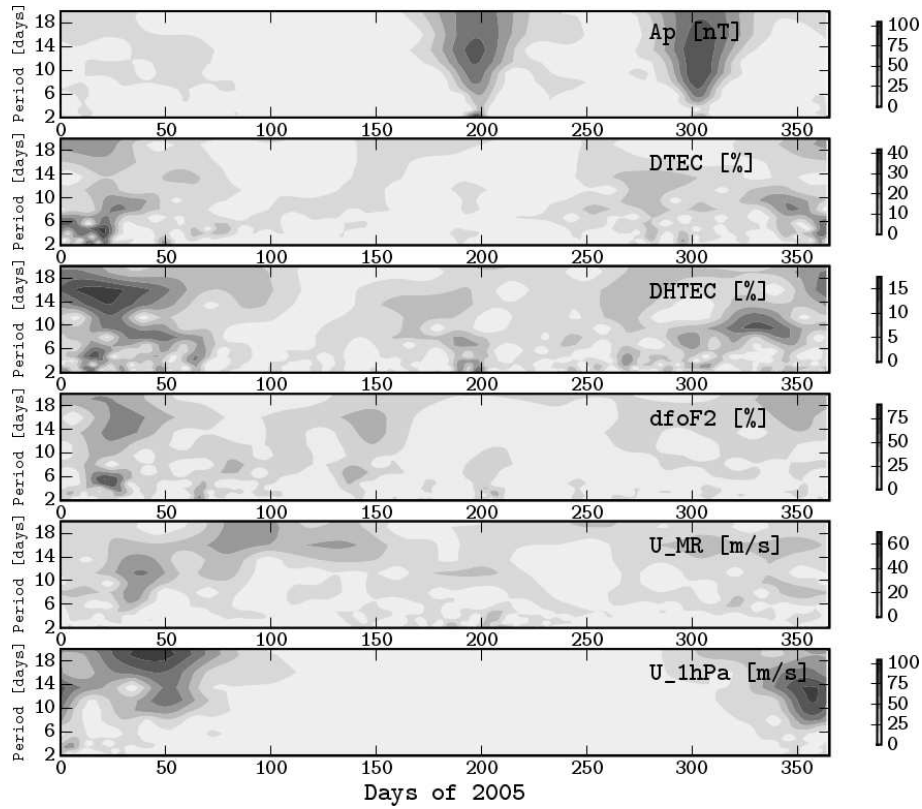


Figure 5: Wavelet spectra of 2005 calculated for the following data:  $A_p$ , DTEC, DPTEC,  $df\ of\ F2$ ,  $U_{MR}$ ,  $U_{1hPa}$ .

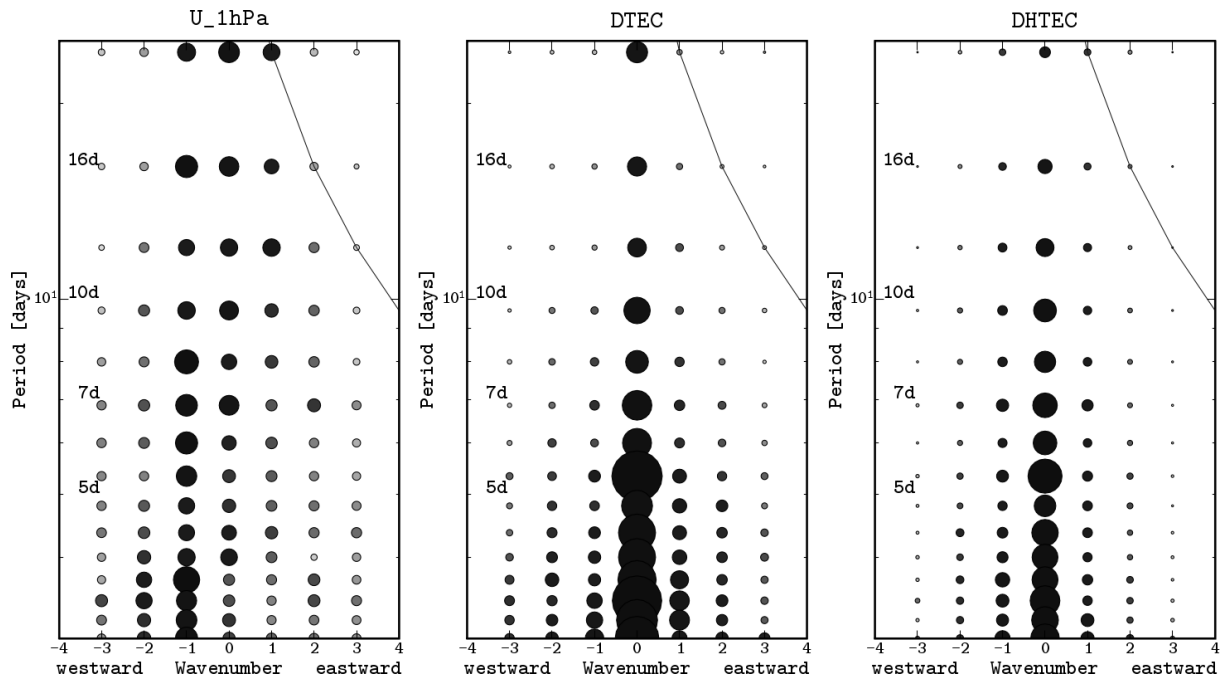


Figure 7: Averaged period-wavenumber spectra of stratospheric  $U_{1hPa}$  and ionospheric DTEC and DHTEC represent the mean amplitude of each separated wave type.

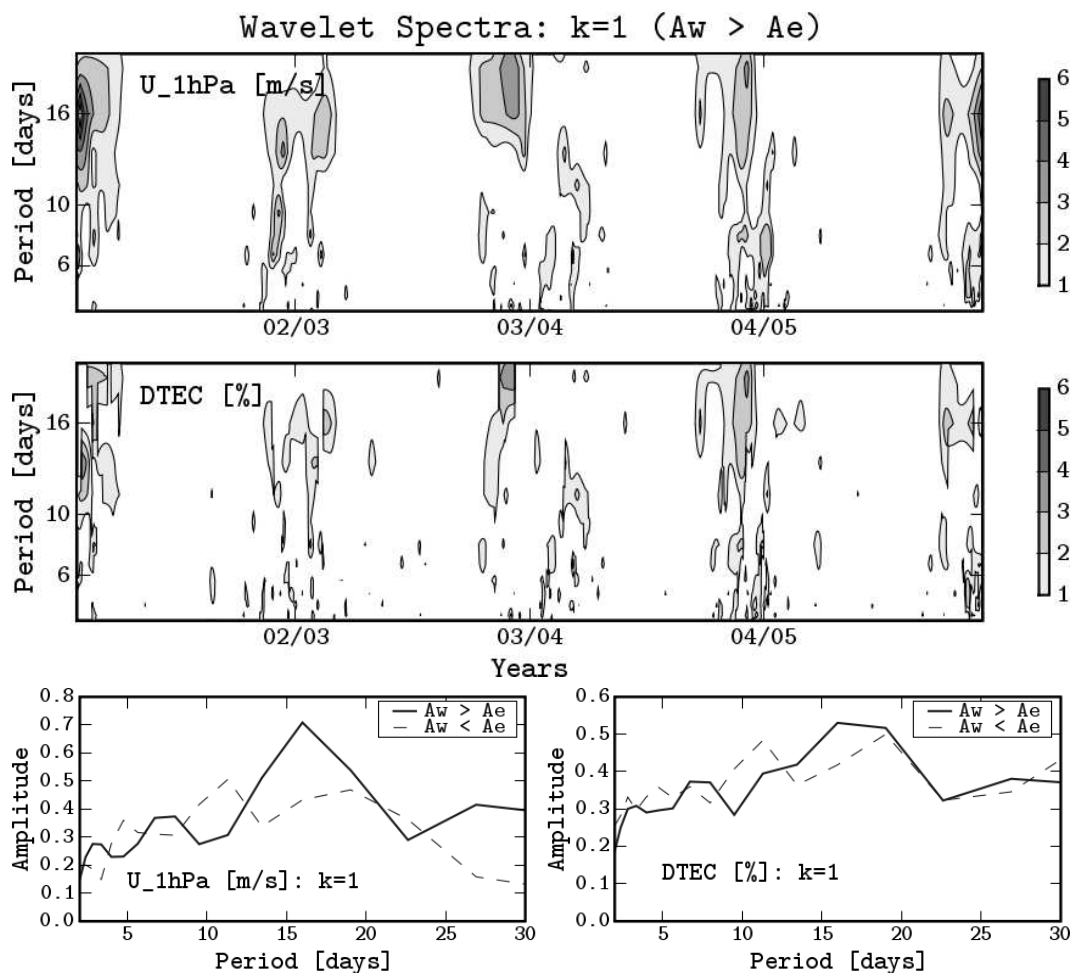


Figure 8: Wavelet spectra of the pure planetary wave ( $A'_w$ ) westward propagating ( $k=1$ ) for the stratosphere ( $U_{1hPa}$ ) and the ionosphere ( $DTEC$ ), which is calculated from the difference between the westward- and eastward propagating wave amplitudes ( $A_w > A_e$ ). The lower panel show the averaged spectra for the west- and eastward travelling waves.

## 6 Discussion and Outlook

Information of the neutral upper atmosphere variability can be derived from the ionospheric total electron content (TEC) based of GPS measurements, which provide a unique global coverage of the ionosphere. The application of filter techniques and spectral analysis in space and time eliminates especially the solar dependency from ionospheric disturbances and reveals the background climatology of the thermosphere (tidal winds, meridional circulation), which causes anomalies (daily, seasonal) in TEC. Signatures of PW type oscillations from below are also expected in the normalised signal of ionospheric disturbances through indirect mechanisms of modulation. For excluding the solar cycle from ionospheric disturbances several differential TEC values ( $DTEC$ ,  $DHTEC$ ,  $DPTEC$ ) were introduced using different references (monthly median, lowpass filter, local time transform).

The result from spectral analysis of times series over  $52^\circ\text{N}/12^\circ\text{E}$  and several middle and upper atmospheric layers (Fig. 5) shows a good correspondence in the seasonal variability of wave type

oscillations.

PW at stratospheric heights (1hPa) are predominately westward propagating having zonal wavenumber  $k=1$  and periods of quasi 4-, 7-, 16-days (Fig.7, left panel). At northern hemisphere mid-latitudes the maximum of PW activity occurs in winter. PW type oscillations in the ionosphere are more variable over the season. In the averaged period-wavenumber spectrum the amplitudes for west- and eastward propagating component are equivalent and strong for  $k=1$ . But the elimination of the standing part from travelling components by calculating the difference reveal simultaneous observations of periods close to the atmospheric normal modes. Dependent on the used normalisation method a stationary part is visible (*DPTEC, DHTEC*) or excluded (*DTEC*).

This study has shown that signatures of PW, which carry meteorological information from below, can be extracted from ionospheric total electron content variability. Further studies must be performed for validation and measurements from satellites as well as the numerical modelling will play an essential role to understand the physical processes of vertical coupling.

## Acknowledgements

This study was supported by Deutsche Forschungsgemeinschaft under grant JA 836/19-1 within the special priority program SPP 1176 "CAWSES" and by RBFR under grant RFBR-DFG 05-05-04001. The TEC data are produced by DLR Neustrelitz. The geomagnetic and solar indices have been provided by NOAA, Solar-Terrestrial Physics Division, the stratospheric reanalysis data by UK Met Office through BADC and the ionosonde data at Juliusruh observatory by J. Mielich from Institute for Atmospheric Physics (IAP). Special thanks to the DLR-IMF, Oberpfaffenhofen, for financial support.

## References

- [1] Altadill, D., Apostolov, E. M., Jacobi, C., Mitchell, N. J., 2003: Six-day westward propagating wave in the maximum electron density of the ionosphere, *Ann. Geophysicae*, 21, 1577-1588.
- [2] Beard, A.G., Williams, P. J. S., Mitchell, N. J., Muller, H. G., 2001: A spectral climatology of planetary waves and tidal variability, *J. Atmos. Solar-Terr. Phys.*, Vol. 63, pp. 801-811.
- [3] Borries, C., Jakowski, N., Jacobi, Ch., Hoffmann, P., Pogoreltsev, A., 2007, Spectral analysis of planetary waves seen in the ionospheric total electron content (TEC): First results using GPS differential TEC and stratospheric reanalyses, *J. Atm. Sol.-Terr. Phys.*, doi:10.1016/j.jastp.2007.02.004.
- [4] Forbes, J. M., 1996, Planetary waves in the thermosphere-ionosphere system, *J. Geomagn. Geoelect.*, Vol. 48, pp. 91-98.
- [5] Gordienko, G. I., Aushev, V. M., Fedulina, I. N., Ryazapova, S. Sh., Shepherd, M. G., 2005, Observation of the F2-Layer variability from the "Alma-Ata" observatory, *J. Atm. Sol.-Terr. Phys.*, Vol. 67, pp. 563-580.
- [6] Hagan, M. E., Forbes, J. M., Vial, F., 1993, Numerical investigation of the propagating of the quasi 2-day wave into the lower thermosphere, *J. Geophys. Res.*, Vol. 98, pp. 23193-23205.

- [7] Hayashi, Y., 1971, A General Method of Resolving Disturbances into Progressive and Retrogressive Waves by Space Fourier and Time Cross-Spectral Analyses, *J. Meteor. Soc. Japan*, Vol. 49, pp. 125-128.
- [8] Hoffmann, P., Jacobi, Ch., 2007, Response of the ionospheric total electron content to stratospheric normal modes, *Wiss. Mit. Inst. Meteorol. Univ. Leipzig*, Vol. 41, 57-68.
- [9] Jacobi, Ch., Fröhlich, K., Pogoreltsev, A. I., 2006, Quasi two-day wave modulation of gravity wave fluxes and the consequence for planetary wave propagation in a simple general circulation model, *J. Atmos. Sol.-Terr. Phys.*, Vol. 68, pp. 283-292.
- [10] Jacobi, Ch., Jakowski, N., Pogoreltsev, A. I., Fröhlich, K., Hoffmann, P., Borries, C., 2007, The CPW-TEC project: Planetary waves in the middle atmosphere and ionosphere, *Adv. Radio Sci.*, Vol. 5, pp. 393-397.
- [11] Lastovicka, J., 2006, Forcing of the ionosphere by waves from below, *J. Atmos. Sol.-Terr. Phys.*, Vol. 68, pp. 479-497.
- [12] *Numerical Recipes in C: The Art of Scientific Computing*, by Flannery, Press, Teukolsky, and Vetterling, Cambridge University Press, Cambridge, MA, 1988.
- [13] Pancheva, D., Mitchell, N., Clark, R. R., Drojbeva, J., Lastovicka, J., 2002, Variability in the maximum height of the ionospheric F2-Layer over Millstone Hill (September 1998 - March 2000) influence from below and above, *Ann. Geophysicae*, Vol. 20, pp. 1807-1819.
- [14] Pogoreltsev, A. I., Pancheva, D., Mitchell N. J., 2002, Secondary planetary waves in the middle atmosphere: numerical simulation and analysis of the neutral wind data, *J. Atm. Sol.-Terr. Phys.*, Vol. 64, pp. 1251-1261.
- [15] Pogoreltsev, A. I., Vlasov, A. A., Fröhlich, K., Jacobi, Ch., 2007, Planetary Waves in coupling the lower and upper atmosphere, *J. Atm. Sol.-Terr. Phys.*, Vol. 69, pp. 2083-2101.
- [16] Salby, M. L., 1984, Survey of planetary-scale traveling waves: The state of theory and observations, *Rev. Geophys. Space Phys.*, Vol. 22(2), pp. 209-236.
- [17] Swinbank, R., O'Neill, A., 1994, A stratosphere-troposphere data assimilation system, *Monthly Weath. Rev.*, Vol. 122, pp. 686-702.
- [18] Torrence, Ch., Compo, G. P., 1998, A practical guide to wavelet analysis, *Bulletin American Meteorol. Soc.*, Vol 79, pp. 61-78.

## **Author's address**

Peter Hoffmann  
Institute for Meteorology  
Stephanstr. 3  
04103 LEIPZIG

email: phoffmann@uni-leipzig.de